Thin Solid Films 601 (2016) 80–83

Contents lists available at ScienceDirect

Thin Solid Films

journal homepage: www.elsevier.com/locate/tsf

Pyroelectricity of $Pb(Zr_{0.52}Ti_{0.48})O_3$ films grown by sol–gel process on silicon

R. Moalla [a], G. Le Rhun [b], E. Defay [b,c], N. Baboux [d], G. Sebald [e], R. Bachelet [a,*]

[a] Institut des Nanotechnologies de Lyon, INL-CNRS UMR 5270, Ecole Centrale de Lyon, Bâtiment F7, 36 av. Guy de Collongue, 69134 Ecully Cedex, France
[b] CEA, LETI, MINATEC Campus, 17 Rue des Martyrs, 38054 Grenoble, France
[c] Luxembourg Institute of Science and Technology (LIST), Materials Research & Technology Department (MRT), 41 Rue du Brill, L-4422 Belvaux, Luxembourg
[d] Institut des Nanotechnologies de Lyon, INL-CNRS UMR 5270, INSA de Lyon, Bâtiment Blaise Pascal, 7 avenue Jean Capelle, 69621 Villeurbanne Cedex, France
[e] Laboratoire de Génie Electrique et Ferroélectricité, LGEF EA 682, INSA de Lyon, Bâtiment Gustave Ferrié, 8 rue de la Physique, 69621 Villeurbanne Cedex, France

ARTICLE INFO

Article history:
Received 5 June 2015
Received in revised form 23 October 2015
Accepted 28 October 2015
Available online 29 October 2015

Keywords:
Pyroelectricity
Lead zirconate titanate
Integration on silicon
Sol–gel process

ABSTRACT

Pyroelectric $Pb(Zr_{0.52}Ti_{0.48})O_3$ films have been grown by sol–gel process on Si(001). Intrinsic pyroelectric coefficient has been measured through ferroelectric loops recorded at different temperatures and is about $-300\ \mu C/m^2K$. Corresponding converted pyroelectric power density is estimated to be ~1 mW/cm^3 for a temperature variation of 10 °C every 6 s. Pyroelectric response of these films has been confirmed by direct measurements of the pyroelectric current with temperature variations at zero electric field. These results are of high interest for integrated thermally-sensitive devices.

1. Introduction

Pyroelectric films can deserve many devices such as detectors, imaging tools, biosensors, *thermal-electric* energy converters for electricity generation by thermodynamic Olsen cycles or cooling applications by electrocaloric effects [1–3]. Very active researches are currently being carried out to define smart solutions to harvest energy, and in particular to realize self-powered autonomous systems [2,4]. In the microelectronic field, ever more compact devices lead to considerable thermal energy waste. The most famous way to generate electricity from thermal energy is to use thermoelectric materials (Seebeck effect, from thermal gradients in heavily doped semiconductors) [5,6]. However, thermoelectric materials are not optimized for micro- and nano-scales yet [6]. In addition to optimize both *p*- and *n*-doped materials, maintaining significant thermal gradients across the films is a serious drawback in miniaturized systems. An alternative way is to use pyroelectric materials that can produce electricity from temporal variations of temperature, without the requirement of maintaining consequent thermal gradients. Pyroelectric films, that can moreover reach larger efficiencies than thermoelectric materials [7], appear as good candidates for thermal energy harvesting and electricity generation in microelectronic devices. However, the knowledge of the pyroelectric properties and their control is still limited, compared to other properties of ferroelectric materials such as piezoelectricity. Most of the pyroelectric studies reported in literature until now have been carried out on bulk materials and/or with restricted compositions deposited by costly vacuum techniques [1,2,7].

$PbZr_xTi_{1-x}O_3$ (PZT (x:1-x)) is one the ferroelectric oxides with the highest pyroelectric coefficients (p) and figures of merit for pyroelectric energy conversion [1–4,7–8]. However, the pyroelectric properties of this material are sparsely reported and still not optimized in thin films for thermal energy harvesting applications. Pyroelectric properties have been mainly reported for PZT (20:80) epitaxially grown by pulsed laser deposition on matched perovskite oxide substrates [9], whereas the PZT (52:48) composition, substrate with a different thermal expansion coefficient and lower-cost elaboration technique would be of better choice for improved pyroelectric devices. It has been reported for bulk materials that pyroelectric energy conversion efficiency is exalted in the vicinity of phase transitions, where dielectric properties are strongly affected by temperature variations [7], including the case of ferroelectric oxide compositions near a morphotropic phase boundary (MPB) such as PZT (52:48) [10,11]. In addition, pyroelectric responses of PZT films can be enhanced by a large secondary pyroelectric effect when deposited on substrates with different thermal expansion coefficients [1,2,9]. Silicon appears as an appealing substrate since it is a key platform in the microelectronic field and since its thermal expansion coefficient (TEC) is different from that of PZT (TEC = 2.6 and 11 $10^{-6}\ K^{-1}$, for Si and PZT, respectively) [12–14].

* Corresponding author.
E-mail address: romain.bachelet@ec-lyon.fr (R. Bachelet).

http://dx.doi.org/10.1016/j.tsf.2015.10.073
0040-6090/

Here, we report the elaboration and pyroelectric properties of low-cost sol–gel processed PZT (52:48) films on silicon. Intrinsic pyroelectric coefficient is found to be in the range of the bulk value ($-300\ \mu C/m^2K$), and large pyroelectric response has been confirmed by direct measurements of the pyroelectric current through heating and cooling the film at zero electric field.

2. Experimental details

PZT (52:48) films (~500 nm thick) were grown by sol–gel process in a metal–insulator–metal (MIM) capacitor structure on Si(001) substrate. Pt is used as bottom electrode and 100 nm thick layers are deposited by magnetron sputtering at 450 °C, after the sputtering deposition of 10 nm of Ti adhesive layer on thermal SiO_2 and an oxidation annealing at 750 °C. Excess of lead is used in the solution (PZT 110/52/48, provided by Mitsubishi Materials Corporation) to compensate its volatility during the subsequent crystallization annealing. The sol–gel process includes spin coating of 3 layers, each one calcinated on hotplate at 350 °C under air and subsequent crystallization by rapid thermal annealing at 700 °C under oxygen. This step is repeated three times to reach the desired PZT thickness of ~540 nm [15,16]. X-ray diffraction (XRD) was used to investigate the crystalline structure and orientation of the layers. The top electrode is made of 100 nm-thick sputtered Ru. Square-shaped top-contact electrodes were realized by UV-lithography process followed by Ru wet etch with NaOCl. Dielectric properties were investigated through capacitance versus electric field (C–V) measurements at 100 kHz in planar capacitor geometry. The intrinsic pyroelectric properties were determined by measuring ferroelectric hysteresis loops (polarization versus electric field, P–E) at different stabilized temperatures from 20 °C to 120 °C, and direct pyroelectric measurements were done by heating and cooling the sample between room temperature and 110 °C in short-circuit configuration and under zero electric field. The used top-contact sizes range from $280 \times 280\ \mu m^2$ for C–V and P–E measurements to $5 \times 5\ mm^2$ for direct pyroelectric measurements.

3. Results and discussion

An XRD 2θ/ω scan of these heterostructures is displayed in Fig. 1. The PZT film is a single perovskite phase, polycrystalline, with a large majority of {001}-orientation (polycrystalline contribution is estimated to be ~1%). The Pt layer is (111)-oriented, with respect to its densest planes, as observed elsewhere [8]. The measured lattice parameter of PZT along the out-of-plane direction is 4.062 Å, which is close to that of its rhombohedral phase, or that can correspond to the tetragonal phase with a mixture of *a*- and *c*-domain orientation. Although these experimental results do not allow us to precisely define the structure, a remnant polarization should be measured in this MIM planar capacitor stack since an out-of-plane component of the polarization exists whatever these structural configurations. Dielectric properties were analyzed by C–V measurements and the resulting relative dielectric constant (ε_r) of the PZT is then plotted versus electric field in Fig. 2(a). The curve is butterfly shaped, typical of ferroelectric films in MIM structure due to their hysteretic behavior, attesting the ferroelectricity of the PZT films. ε_r is close to 1200 at zero electric field, that is in the range of the highest reported values for this PZT composition and is consistent with previous studies on gradient-free PZT (52:48) films grown by sol–gel process [17,18]. ε_r has been measured at different temperatures from 20 °C to 120 °C (Fig. 2(b)) and increases slightly with temperature up to 1400, in agreement with other studies [15]. It is worth to note that ε_r however remains almost constant in the explored temperature range at high electric fields (between 365 at 20 °C and 390 at 120 °C, under 250 kV/cm, not shown here).

The ferroelectric hysteresis loops (P–E) measured at different temperatures (from 20 °C to 120 °C) are shown in Fig. 3(a). The remnant electric polarization (P_r) is 18.5 $\mu C/cm^2$ at room temperature. As expected, the polarization decreases with increasing temperature and P_r is 13.8 $\mu C/cm^2$ at 120 °C. The resulting saturation polarization under high electric field (900 kV/cm) is plotted versus temperature in Fig. 3(b). The saturation polarization decreases linearly with temperature, as expected for this range of temperature and electric field (far from Curie temperature and in the Q vs E linear region) [1,2,19]. The slope of the linear fit gives the mean intrinsic pyroelectric coefficient (*p*) of the film in this temperature range [1,2,19], that is found to be

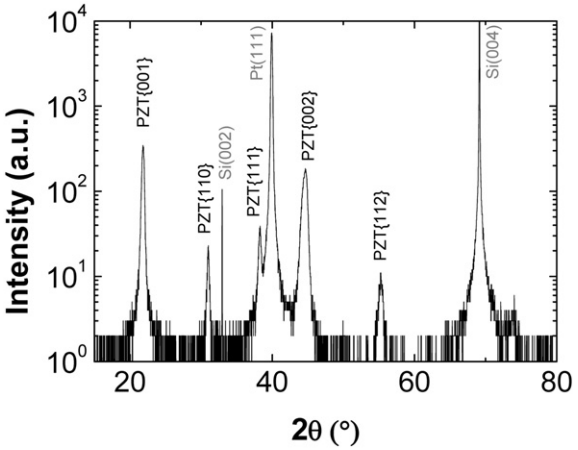

Fig. 1. XRD 2θ/ω scan of the PZT/Pt/TiO_x/SiO_2/Si(001) heterostructure.

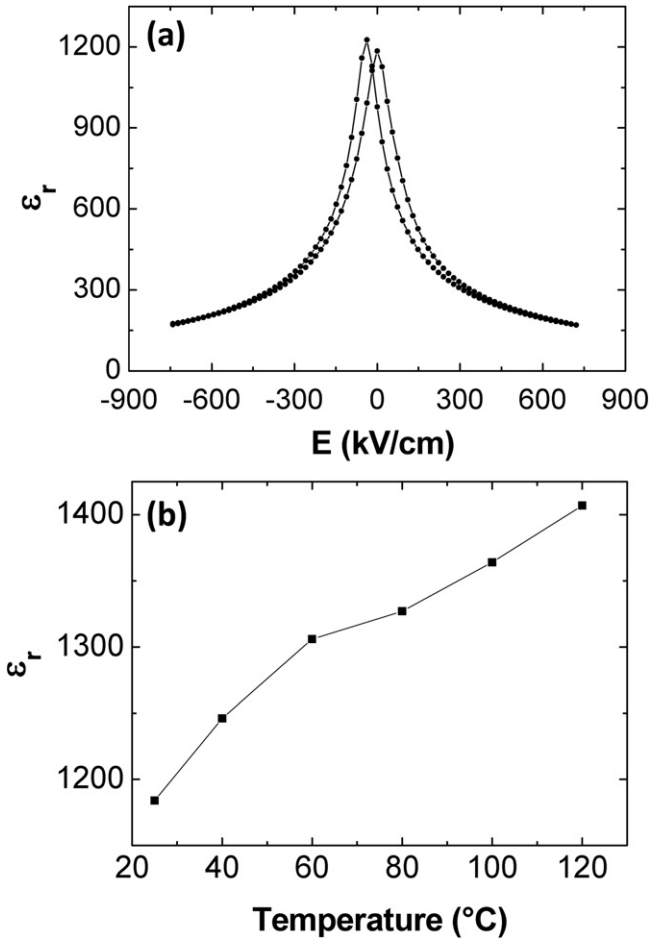

Fig. 2. (a) Dielectric constant versus electric field from C–V measurements. (b) Dielectric constant (maximum at zero electric field) versus temperature from C–V measurements at different sample temperatures from 20 °C to 120 °C.